JOURNAL OF SOLID STATE CHEMISTRY 107, 471–479 (1993)

Chromium Site Specific Chemistry and Crystal Structure of $LiCaCrF_6$ and Related Chromium Doped Laser Materials

BERNHARD RUPP,* WAYNE L. KWAY, AND JOE WONG

Lawrence Livermore National Laboratory, University of California, Livermore, California 94551

PETER ROGL

Institut für Physikalische Chemie, Währingerstrasse 42, A-1090 Vienna, Austria

AND PETER FISCHER

Labor für Neutronenstreuung ETHZ & PSI, CH-5232 Villigen PSI, Switzerland

Received June 8, 1992; accepted April 9, 1993

The crystal structure of $LiCaCrF_6$, a fully Cr-substituted lithium metal hexafluoride representative of laser materials with the generic formula $LiMe^{II}Me^{III}_{1-x}Cr_xF_6$ (Me^{II} = Ca, Sr; Me^{III} = Al) was determined by X-ray single crystal diffraction and neutron powder profile refinement. $LiCaCrF_6$ was confirmed as a $LiCaAlF_6$ (Colquiirite)-type (space group $P\bar{3}1c$ (No. 163), $Z = 2$, $a = 5.1054(08)$ Å, $c = 9.7786(10)$ Å, Li in 2*c*, Ca in 2*b*, Cr in 2*d*, and F in 12*i* with x,y,z of 0.3652(3), 0.0183(4), 0.1402(1)). Deviation from centrosymmetry ($P31c$; No. 159) and full occupation were examined and appear to be insignificant. We selected $LiCaCrF_6$ as a model compound for the determination of EXAFS phase shifts to provide Cr site specific information in 3% Cr-doped $LiCaAlF_6$ laser crystals where Cr occupies a slightly distorted CrF_6 octahedron with a Cr–F distance (1.89(8) Å) practically identical to Cr–F in $LiCaCrF_6$ (1.901 Å) and CrF_3 (1.899 Å). The pseudobinary laser material $LiSrAl_{1-x}Cr_xF_6$ forms a true solid solution over the complete composition range $0 \leq x \leq 1$.

1. Introduction

Chromium-doped lithium metal hexafluorides (LMHF) of the general formula $LiMe^{II}Me^{III}_{1-x}Cr_xF_6$ (Me^{II} = Ca, Sr; Me^{III} = Al) gained considerable interest as a promising class of new solid state laser materials with a wide tuning range (*1*) ($LiCaAlF_6:Cr^{3+}$), and very recently in a newly developed 752-nm wing-pumped laser design (*2*) with high Cr-doping ($LiSrAl_{1-x}Cr_xF_6$, $x \geq 0.15$). The structure of the laser host material $LiCaAlF_6$ (Colquiirite) and the cell constants for some isotypic compounds have been determined earlier (*3*). No crystal data for a fully chromium-substituted LMHF have been reported so far (*4*), however, and crystallographic data on the solid solution $LiSr(Al,Cr)F_6$ are not available as well. In view of the reported uncertainty of the $LiCaCrF_6$ structure (*5*) and the large variety of possible LMHF structure types (*3, 6*), we elected to determine the crystal structure of this fully chromium-substituted LMHF. In addition, $LiCaCrF_6$ can serve as a model substance providing information necessary for the determination of the chromium environment in slightly doped $LiCaAlF_6:Cr^{3+}$ by means of Extended X-ray Absorption Fine Structure (EXAFS). The local Cr–F geometry is of

* To whom correspondence should be addressed.

0022-4596/93 $5.00

TABLE I

CRYSTALLOGRAPHIC DATA FOR $LiCaCrF_6$ AS DETERMINED BY SINGLE-CRYSTAL X-RAY DIFFRACTION

Compound	$LiCaCrF_6$
Formula units per unit cell	$Z = 2$
Lattice constants	$a = 5.1042$ Å, $c = 9.7767$ Å
Space group	$P\bar{3}1c$ (No. 163), origin at $\bar{1}$
Formula weight	213.0 g · mol^{-1}
Calculated X-ray density	$\rho_c = 3.207$ g · cm^{-3}
Absorption coefficient	μ(Mo $K\alpha$) = 36.0 cm^{-1}
Crystal dimensions	50 × 60 × 120 μm
$\theta/2\theta$ scans up to	$2\theta = 70°$
Range in hkl	±8, 8, ±16
Total number of reflections	2137
Unique reflections	333
Absorption correction	from ψ scans
Transmission coefficient	1.204 (highest/lowest)
Inner residual	$R_{int} = 0.074$
Reflections with $I > 3\sigma I$	304
Number of variables	16
Conventional residual	$R_F(F_o) = 0.045$
Weighted residual	$R_w(F_o) = 0.036$
Weights	$w = 1/\sigma^2$
Scale factor	1.2232(89)

Atom	Position	n	x	y	z	U_{11}	U_{22}	U_{33}	U_{12}	U_{13}	U_{23}
Ca	2*b*	2.0	0	0	0	0.0112(4)	0.0112(4)	0.0080(4)	0.0056(2)		
Li	2*c*	2.0	1/3	2/3	1/4	0.0149(22)					
Cr	2*d*	2.0	2/3	1/3	1/4	0.0083(3)	0.0083(3)	0.0085(3)	0.0041(2)		
F	12*i*	12.0	.3652(3)	.0183(4)	.1402(1)	0.0139(7)	0.0124(7)	0.0142(6)	0.0051(5)	−.0053(5)	−.0016(4)

Note. Numbers in parentheses give the estimated standard deviations σ of the last significant digits of refined parameters.

interest as asymmetric distortions in the local symmetry at the chromium site appear to reduce the adverse excited state absorption (7) in $LiCaAlF_6:Cr^{3+}$.

2. Experimental

2.1. Materials Preparation

Crystals have been grown using the zone-melting (ZM) technique from starting materials prepared by reactive atmosphere processing (RAP) using hydrogen fluoride as the reactive gas. The RAP and ZM techniques and the equipment used have been reported previously in detail (8) and are described briefly as follows.

The starting materials LiF and AlF_3 were both high-purity, optical grade materials from Johnson Matthey or GFI Advanced Technologies; CrF_3 was the high-purity, ultra-dry grade from APL Engineering Materials. From these components, a precursor material for the crystal growth was prepared by the standard RAP technique. The charges were prereacted in a platinum boat, heated to 800°C, and soaked at this temperature in an HF atmosphere for 4 hr. The prereacted RAP material was then zone refined in a graphite boat under argon atmosphere at a temperature of 850°C and a zone rate of 3 mm/hr. DTA (Differential Thermal Analysis) measurements displayed narrow and single melting and solidification peaks indicative of congruent melting and single phase nucleation.

2.2. X-Ray and Neutron Diffraction

A small fragment from a large, zone-melted $LiCaCrF_6$ single crystal was selected for the single-crystal X-ray diffraction study. Larger parts of the same crystal were powdered to a grain size smaller than 30 μm to minimize effects of preferred orientation, and were sealed under helium in the 8 × 50-mm cylindrical vanadium sample con-

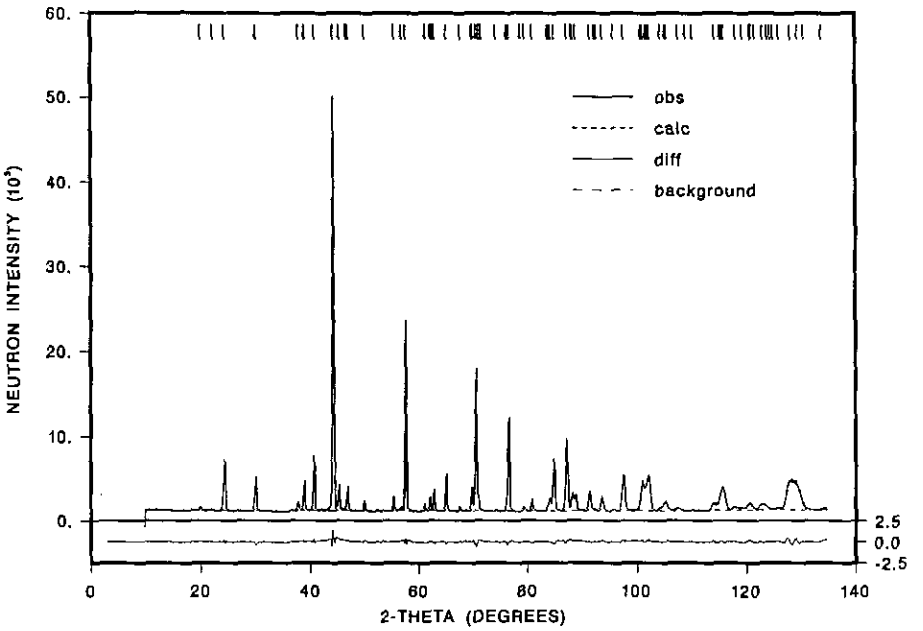

FIG. 1. Neutron powder diffraction pattern of $LiCaCrF_6$ (295 K, λ = 1.7012 Å). (—) Observed, (---) calculated, (—) difference, and (—·—) background values.

tainer used in the neutron diffraction experiment.

The single crystals were initially oriented along [001] and were examined by means of Cu $K\alpha$ Weissenberg photographs. X-ray intensity data were collected on an automatic Stoe 4-circle diffractometer in one hemisphere of the reciprocal space (sin $\theta/\lambda \leq 0.8$ Å^{-1}) using monochromatized Mo $K\alpha_1$ radiation (for details refer to Table I). Precise cell constants were obtained by least-squares refinement (*9*) of Guiner powder film data (≥20 reflections, focusing 114-mm Guinier–Huber camera, monochromatized Cu $K\alpha_1$ radiation). High-purity germanium (99.9999%, a_0(293 K) = 5.657906 Å) was added to the sample powder as an internal calibration standard.

Neutron diffraction data were collected at 295 K on the DMC multidetector powder diffractometer (*10*) at the 10 MW SAPHIR reactor in Villigen, PSI, Switzerland (LN_2-cooled Si filter, vertically focusing Ge (311) monochromator, collimation 10′/–/12′, wavelength 1.7012(5) Å). The diffraction patterns were refined employing the Rietveld method (*11*) using a modified code by Hewat (*12*) including options for anisotropic temperature factor refinement. Neutron scattering lengths and absorption cross sections were taken from a recent compilation by Sears (*13*); no absorption correction had to be applied for $LiCaCrF_6$.

2.3. X-Ray Absorption

Chromium K-edge EXAFS spectra were recorded on beamline X-11A at the Brookhaven National Synchrotron Light Source. The X-ray storage ring was operated at 2.53 GeV with electron beam currents of 120 to 160 mA. Silicon (111) monochromator crystals were used in combination with entrance slit widths of 0.5 mm, providing an energy resolution of about 0.5 eV at 5.7 keV. Powders of sample material were sealed in Kaptan tape or prepared as DUCO films to obtain transmission samples of uniform thickness corresponding to 1 to 2 absorption lengths. The $LiCaCrF_6$ sample was examined in conventional transmission geometry

TABLE II

STRUCTURAL PARAMETERS OF $LiCaCrF_6$ AT ROOM TEMPERATURE AS OBTAINED FROM NEUTRON POWDER PROFILE ANALYSIS

Space group $P\bar{3}1c$ (No. 163)						
Atom	Position	x	y	z	B	n
Ca	2*b*	0	0	0	0.54(11)	1.92(5)
Li	2*c*	1/3	2/3	1/4	0.57(26)	2.01(7)
Cr	2*d*	2/3	1/3	1/4	0.57(14)	2.00[a]
F	12*i*	.3662(3)	.0192(4)	.1405(1)	0.93(03)	11.85(18)
$R_I = 3.1$, $R_{wp} = 7.2$, $R_e = 3.3$, $\Psi^2 = 5.6$						

Space group $P31c$ (No. 159)						
Atom	Position	x	y	z	B	n
Ca	2*a*	0	0	.0000[a]	0.39(12)	1.90(5)
Li	2*b*	1/3	2/3	.2561(81)	0.64(30)	1.99(7)
Cr	2*b*	2/3	1/3	.2500[a]	0.50(15)	2.00[a]
F(1)	6*c*	.3613(15)	.0020(21)	.1464(18)	0.56(20)	5.86(23)
F(2)	6*c*	.6466(16)	.0018(23)	.3658(19)	1.31(26)	5.94(25)
$R_I = 2.8$, $R_{wp} = 6.5$, $R_e = 3.3$, $\chi^2 = 4.8$						

Note. Numbers in parentheses give σ of the last significant digits of refined parameters; reliability factors were evaluated as defined in Ref. (*23*). Data for the centrosymmetric spacegroup $P\bar{3}1c$ (No. 163) as well as for $P31c$ (No. 159) are listed for comparison. A significance test evaluating the differences in the profile description revealed that the acentric model is not significantly better beyond a significance level of 70%. Neutron wavelength $\lambda = 1.7012$ Å. Units for B: Å^2, isotropic temperature factors of the form $e^{(-B_{iso}\sin^2\theta/\lambda^2)}$. Cell constants (Å): $a = 5.1054(8)$, $c = 9.7786(10)$.

[a] When refined individually, these parameters remained within less than one σ. They were thus held fixed in subsequent refinement cycles.

(high Cr concentration) and the 3% Cr-doped $LiCaAlF_6$ in fluorescence mode (*14*) using a Lytle-type (*15*) detector. Chromium (1-μm Cr on Al foil) was simultaneously scanned as an energy calibration reference during each measurement.

3. Results and Discussion

3.1. Crystal Structure of $LiCaCrF_6$

Weissenberg [001] photographs revealed trigonal, high Laue symmetry and the only extinction observed for $(hh2\bar{h}l) = 2n + 1$ indicated $P31c$ (No. 159), and $P\bar{3}1c$ (No. 163) as the possible space groups. A first structural model was obtained using direct methods. As the statistical tests indicated the absence of a center of symmetry, the structural model was initially refined in the noncentrosymmetric space group $P31c$ employing the STRUCSY program package (*16*).

R_F-values at this stage were not better than $R_F = 0.053$ and $R_w = 0.040$, essentially confirming the atom arrangement as derived for centrosymmetric $LiCaCrF_6$. The low-scattering Li atoms were not convincingly revealed from a difference Fourier map ($F_{obs} - F_{CaCrF_6}$); however, when placed in the central voids of the F_6-octahedra, the Li atoms adopted reasonable isotropic temperature factors and a significant deficiency on one of the F sites ($n_{occ} = 0.89$) was observed. The low residual values are in contrast to the statement of Viehbahn that a model derived from a double stacking of a Li_2ZrF_6-type cell (*17*) with alternate Li and Al (or Li and Cr) ordering *a priori* excludes the noncentrosymmetric space group $P31c$.

Despite the statistical tests being in favor of a noncentrosymmetric structure, the re-

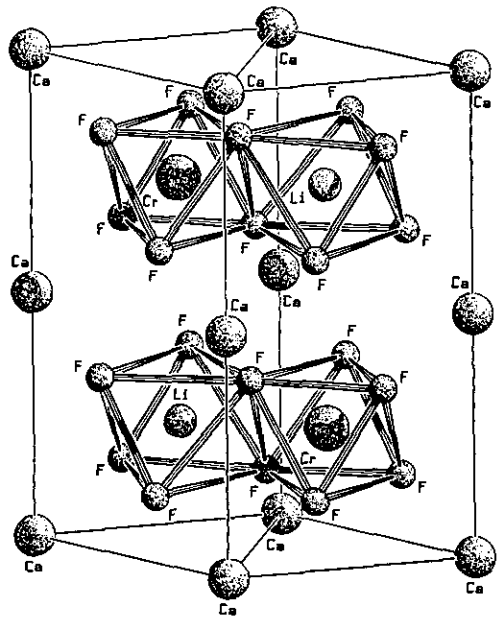

FIG. 2. Crystal structure of $LiCaCrF_6$ which can be described as a network of MeF_6 octahedra with a varying degree of distortion (shown in Table III). The CaF_6 octahedral network is omitted to better emphasize the larger LiF_6 and smaller CrF_6 octahedra. Drawing by the SCHAKAL program (*25*) based on crystal data from this work.

finement in $P\bar{3}1c$ as isotypic with $LiCaAlF_6$ arrived at marginally improved residual values $R_F = 0.045$ and $R_w = 0.036$. The geometrical deviations of the two independent fluorine atoms ($6c_1$ and $6c_2$) in $P31c$ from their ideal position ($12i$) in $P\bar{3}1c$ are very small and do not appear to justify a loss of centrosymmetry. In addition, refinement of the Ca and F atoms revealed no significant deviations from a full occupancy in the centrosymmetric case (see Table I for a complete listing of positional and thermal parameters).

In order to confirm and complement the structural information derived from our X-ray work (especially in regard to the Li atoms, which were not directly accessible in the X-ray single-crystal study) we recorded additional neutron diffraction powder profiles. As the negative neutron scattering length of Li critically determines the accuracy of the refinement of the Li positions, we verified the Li isotope ratio in our samples (and starting material) by means of secondary ion mass spectroscopy (SIMS). We obtained a relative isotope abundance of 8.74(36)% for ^6Li and of 91.26(36)% for ^7Li. Combining the individual scattering lengths for each isotope, an average scattering length $\bar{b}$ of $-1.85(3)$ fm results. This value was used in the profile refinement.

The neutron diffraction profiles (Fig. 1) were refined either in the centrosymmetric space group $P\bar{3}1c$ or in the noncentric in $P31c$ (see Table II for a comparison of the refinement results). In either refinement, all occupational factors remained within less than 2σ of the full occupation (the minute underoccupation at the Ca site is associated with a matching deficiency at the fluorine sites and thus the crystal's charge remains balanced) and both the deviation of the Li z-parameter from its ideal position and the splitting of fluorine $12i$ into two $6c$ positions are marginal. In addition, a significance test evaluating the differences in the profile description (*18*) confirmed that the acentric model is not significantly better beyond a confidence level of about 70%. In accordance with the single-crystal X-ray data, we find thus little justification to presume the acentric space group $P31c$.

3.2. EXAFS Spectroscopy of Chromium Sites

The local Cr environment in very lightly doped (3%) $LiCaAlF_6:Cr^{3+}$ cannot directly be accessed by diffraction methods. In this case EXAFS spectroscopy (*19*) provides a tool to investigate local-site geometry and site-specific chemistry of the chromium ion. In order to extract bond distances from the measured EXAFS signal, the phase shifts for the corresponding central atom and backscattering neighbor atoms must be known. These phase shifts can be obtained experimentally from suitable reference substances of known structure. CrF_3 contains chromium ions in an octahedral environ-

TABLE III

COORDINATION GEOMETRY AND DISTANCE OF FIRST TWO COORDINATION SHELLS IN $LiCaCrF_6$, $LiCaAlF_6$, AND CrF_3 ($R\bar{3}c$, OBVERSE HEXAGONAL SETTING)

Compound	Central atom	Ligand atoms	Coord. No.	Distance (Å)[a]	Bond angles (±0.1°)	Coord. type[b]
$LiCaCrF_6$	Cr (2*d*)	F (12*i*)	6	1.901	176.3, 86.1, 91.3	DO
	Cr (2*d*)	Li (2*c*)	3	2.948	120.0	T
	Li (2*c*)	F (12*c*)	6	2.028	171.8, 79.5, 91.6, 94.7	H
	Li (2*c*)	Cr (2*d*)	3	2.948	120.0	T
	Ca (2*b*)	F (12*i*)	6	2.282	180.0, 87.5, 92.5	DO
	Ca (2*b*)	F (12*i*)	6	3.562	180.0, 73.9, 106.1	TA
$LiCaAlF_6$	Al (2*d*)	F (12*i*)	6	1.800	177.22, 87.2, 90.9, 91.2	DO
	Al (2*d*)	Li (2*c*)	3	2.885	120.0	T
	Li (2*c*)	F (12*c*)	6	2.009	169.6, 76.3, 91.8, 96.4	H
	Li (2*c*)	Al (2*d*)	3	2.885	120.0	T
	Ca (2*b*)	F (12*i*)	6	2.273	180.0, 86.7, 92.5	DO
	Ca (2*b*)	F (12*i*)	6	3.490	180.0, 74.7, 105.3	TA
CrF_3	Cr (6*b*)	F (18*e*)	6	1.899	180.0, 89.8, 90.2	O
	Cr (6*b*)	Cr (6*b*)	6[c]	3.927	180.0, 87.0, 93.0	TA

[a] Due to the imperfect coordination geometry the distances vary slightly for different atoms in one coordination shell. A full listing of individual bond distances and angles and can be easily obtained using the SEXIE program (*24*).

[b] O, nearly ideal octahedron; DO, slightly distorted octahedron; TA, trigonal antiprismatically distorted octahedron; H, severely distorted octahedron; and T, planar triangle.

[c] The second Cr coordination shell in CrF_3 actually comprises an additional F_6 antiprismatic subshell at a slightly larger distance yielding a total coordination number of 12.

ment (*20*) and could be considered a suitable reference substance. In rhombohedral CrF_3, though, the CrF_6-octahedra are connected via their corners, whereas in the complex fluorides of the $LiCaAlF_6$-type the octahedra share a common edge (Fig. 2). For this series of compounds, isotypic $LiCaCrF_6$ serves as an appropriate model substance. For a review of the stability of the different cation ordering in $AMe^{II}Me^{III}F_6$ fluorides as a function of cation size we refer the reader to a series of papers by Courbion and co-workers (see, e.g., Ref. *21*).

We have listed bond distances, bond angles, and coordination information for $LiCaCrF_6$, $LiCaAlF_6$, and CrF_3 in Table III. From a comparison of the next nearest neighbor coordination around Al and Li in $LiCaAlF_6$ one can infer that the second shell looks different depending on whether Cr substitutes an Al or a Li atom, respectively: The second coordination shell comprises Li when Cr is located at an Al (2*d*) site, and Al when Cr occupies a Li (2*c*) position. The small difference in the scattering amplitudes between Li and Al in combination with a low coordination number of 3, however, did not suffice to permit a *direct* determination of the Cr location in $LiCaCrF_6$ by the EXAFS technique.

Nevertheless, the Cr–F distance (1.901 Å) and coordination information obtained from the $LiCaCrF_6$ neutron diffraction data could be used to derive an experimental phase shift for the Cr–F nearest neighbor shell in the X-ray absorption process. This phase shift was used in a phase-corrected Fourier transform for the Cr^{3+} site in $LiCaAlF_6:Cr^{3+}$ to derive the actual Cr–F distance (Fig. 3). We find that the Cr–F distance of 1.89(8) Å in $LiCaAlF_6:Cr^{3+}$ is prac-

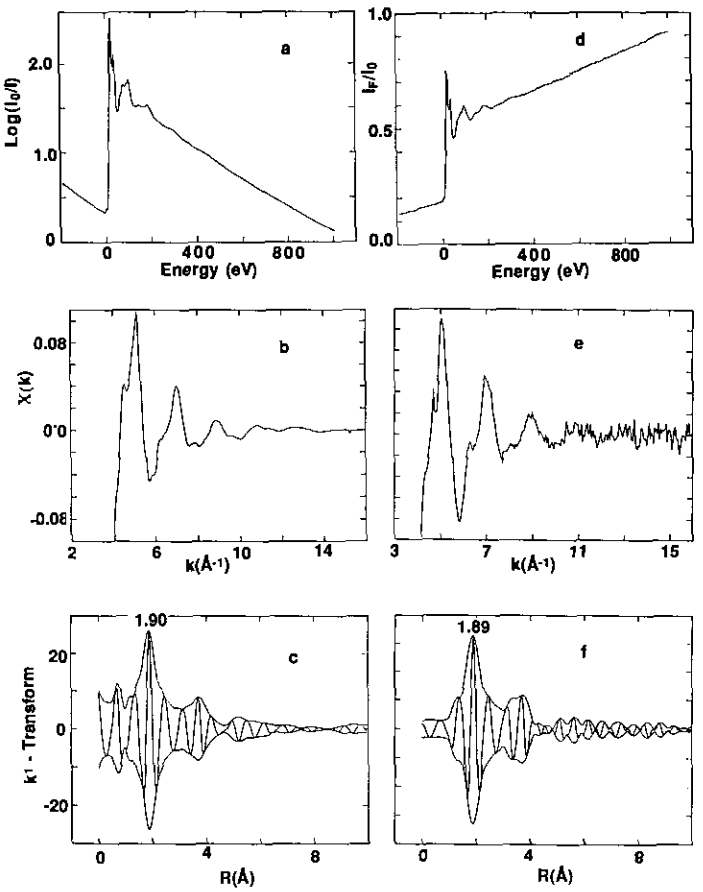

FIG. 3. EXAFS spectra and processed data for $LiCaCrF_6$ (left column, transmission technique) and $LiCaAlF_6:Cr^{3+}$ (right column, fluorescence technique). (a,d) Experimental Cr K-edge EXAFS spectra; (b,e) extracted EXAFS signal plotted as $\psi(k)$ vs wave number k; (c,f) phase-corrected k^1 – Fourier transform of the extracted signal showing the radial distribution of scattering neighbor atom distances around the Cr center. The energy zero in (a,d) was determined by the first inflection point in the derivative spectrum of the Cr metal reference.

tically identical to the Cr–F distance found in the Cr-rich model compound (and in CrF_3 as well), indicating a very stable CrF_6 octahedral configuration in $LiCaAlF_6:Cr^{3+}$ with little distortion even in the case of low chromium doping. The actual degree of the distortion cannot be determined, but from the data in Table III it becomes evident that the "softer" LiF_6 octahedra suffer the most distortion which allows the "harder" CrF_6 octahedra to assume a nearly ideal configuration. In addition to arguments from charge distribution and optical spectroscopy (*1*), this strongly indicates that Cr in fact occupies the 2*d* (Al) sites in $LiCaAlF_6:Cr^{3+}$.

3.3. *Solid Solution LiSr(Al,Cr)F_6*

The existence of a solid solution in the pseudobinary LMHF system $LiSrAlF_6$–$LiSrCrF_6$ was first indicated by DTA and finally verified by X-ray diffraction. A complete analysis of the thermodynamic data and descriptions of the hydrofluorination process and single crystal growth are presented elsewhere (*22*). With the excep-

TABLE IV

SELECTED CELL CONSTANTS OF FLUORIDES $LiMe^{II}Me^{III}F_6$ (Me^{II} = Ca, Sr; Me^{III} = Al, Cr) AND OF $LiSrAl_{1-x}Cr_xF_6$ ($0 \le x \le 1$)

Compound formula	a (Å)	b (Å)	V (Å^3)	c/a	Ref.[a]
$LiCaAlF_6$	4.996	9.636	208.3	1.929	3
$LiCaCrF_6$	5.095	9.720	218.5	1.908	3
$LiCaCrF_6$	5.1042	9.7767	220.59	1.915	SX
$LiCaCrF_6$	5.1054(08)	9.7786(10)	220.73(07)	1.9153(40	ND
$LiSrCrF_6$	5.170	10.34	239.3	2.000	3
$LiSrCrF_6$	5.1764(13)	10.3723(70)	240.69(20)	2.0038(14)	GN
$LiSrAl_{0.2}Cr_{0.8}F_6$	5.1573(10)	10.3384(63)	238.13(17)	2.0046(13)	GN
$LiSrAl_{0.4}Cr_{0.6}F_6$	5.1419(10)	10.3137(45)	236.16(14)	2.0058(10)	GN
$LiSrAl_{0.6}Cr_{0.4}F_6$	5.1208(07)	10.2813(35)	233.48(10)	2.0078(07)	GN
$LiSrAl_{0.8}Cr_{0.2}F_6$	5.1003(19)	10.2396(58)	230.68(21)	2.0076(14)	GN
$LiSrAl_{0.96}Cr_{0.04}F_6$	5.0847(12)	10.2237(52)	228.91(16)	2.0107(11)	GN
$LiSrAlF_6$	5.0838(13)	10.2184(31)	228.71(13)	2.0100(8)	GN
$LiSrAlF_6$	5.084	10.21	228.54	2.008	3

Note. Numbers in parentheses give σ of the last significant digits.

[a] SX, single-crystal X-ray data; ND, neutron powder diffraction; and GN, Guinier powder film technique; all obtained for this work.

tion of one procured "single crystal" with 4% Cr^{3+}-doping, all samples were single phase and the powder diffraction intensities agreed well with those calculated assuming the $LiCaAlF_6$ structure type. Cell constants of the solid solution were refined from the Guinier powder films and are listed in Table IV. No significant deviations from Vegard's law are displayed (Fig. 4) and a truly continuous solid solution exists. The increase of the cell constants with increasing substitution of Al with the larger Cr ions is about 20% more pronounced in the a direction (as indicated by the decreasing c/a ratio in Fig. 4) and can be interpreted in geometric terms: Along the c-axis the $LiMe^{II}Me^{III}CrF_6$ structure is to a large extent determined by the network of Me^{II}–(Ca) octahedra only, while in the a-direction both the Me^{II}– and the $Me^{I,III}$–(Li,Al,Cr) octahedra contribute to the cell dimensions.

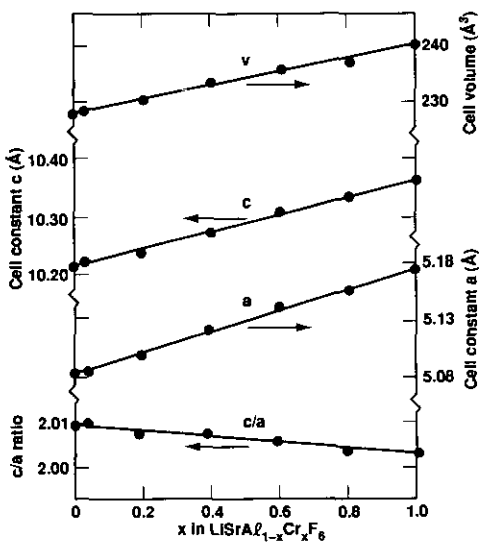

FIG. 4. Variation of cell dimensions vs chromium substitution in the pseudobinary system $LiSrAl_{1-x}Cr_xF_6$. No observable deviations from Vegard's law confirm the existence of an ideal solid solution.

Acknowledgments

This work was sponsored by the U.S. Department of Energy at the Lawrence Livermore National Laboratory under Contract W-7405-Eng-48 and by the PhysiSoft Corporation, Delaware. Thanks are due to Allison Connor, LLNL, for performing the SIMS analyses. We acknowledge the support of the U.S. Department of Energy, Division of Materials Science, under Contract DE-A505-80-ER10742 for its role in the devel-

opment and operation of beamline X-11 at the National Synchrotron Light Source. The NSLS is supported by the Department of Energy, Division of Materials Science and Chemical Sciences Division, under Contract DE-AC02-76CH00016.

References

1. S. A. PAYNE, L. L. CHASE, H. W. NEWKIRK, L. K. SMITH, AND W. F. KRUPKE, *IEEE J. Quantum Electron.* **24**(10), 2243 (1988).
2. S. A. PAYNE, W. F. KRUPKE, L. K. SMITH, W. L. KWAY, L. D. DELOACH, AND J. B. TESSANO, *IEEE J. Quantum Electron.* **28**(4), 1188 (1992).
3. W. VIEHBAHN, *Z. Anorg. Chem.* **386,** 335 (1971).
4. During the preparation of this manuscript we became aware of a preprint by Y. YIN AND D. A. KESZLER, on single crystal structure of additional Colquiirite-type fluorides, *Chem. Mater.* **4,** in press (1992).
5. W. VIEHBAHN, W. RÜDORFF, AND R. HÄNSLER, *Chimia* **23,** 503 (1969).
6. T. FLEISCHER AND R. HOPPE, *Z. Naturforsch. B* **37,** 988 (1982).
7. H. W. H. LEE, S. A. PAYNE, AND L. L. CHASE, *Phys. Rev. B* **39,** 8907 (1989).
8. W. L. KWAY, H. W. NEWKIRK, AND L. L. CHASE, "OSA Proceedings on Tunable Solid-State Lasers, Falmouth, MA, 1989," p. 408.
9. B. RUPP, *Scr. Metall.* **22,** 1 (1988).
10. J. SCHEFER, P. FISCHER, H. HEER, A. ISACSON, M. KOCH, AND R. THUT, *Nucl. Instrum. Methods A* **288,** 477 (1990).
11. H.M. RIETVELD, *J. Appl. Crystallogr.* **2,** 65 (1969).
12. A. W. HEWAT, Report AERE-R7350, Atomic Energy Research Establishment, Harwell, 1973; B. RUPP, MS-DOS microcomputer version (1988).
13. V. F. SEARS, *in* "Methods of Experimental Physics," Vol. **23**(A), "Neutron Scattering" (K. Sköld and D. L. Price, Eds.), p. 521, Academic Press, New York (1986).
14. J. JAKLEVIC, J. A. KIRBY, P. M. KLEIN, A. S. ROBERTSON, G. S. BROWN, AND P. EISENBERGER, *Solid State Commun.* **23,** 697 (1977).
15. F. LYTLE, R. B. GREGOR, D. R. SANDSTROM, E. C. MARQUES, J. WONG, C. SPIRO, C. L. HUFFMANN, AND F. E. HUGGINS, *Nucl. Instrum. Meth. Phys. Res.* **226,** 542 (1984).
16. Program system STRUCSY, Stoe and Cie., Darmstadt, FRG.
17. R. HOPPE AND W. DÄHNE, *Naturwissenschaften* **47,** 397 (1960).
18. E. PRINCE, *Acta Crystallogr. B* **38,** 1099 (1982).
19. J. WONG, *Mater. Sci. Eng.* **80,** 107 (1986).
20. K. KNOX, *Acta Crystallogr.* **13,** 507 (1960).
21. A. HEMON, A. LEBAIL, AND G. COURBION, *Eur. J. Solid State Inorg. Chem.* **27**(6), 905 (1990); A. HEMON AND G. COURBION, *J. Solid State Chem.* **86**(2), 249 (1990).
22. W. L. KWAY, B. RUPP, AND J. B. TASSANO, "10th International Conference on Crystal Growth, San Diego, Aug. 16–21, 1992" *J. Cryst. Growth,* **128,** 1036 (1993).
23. R. A. YOUNG, E. PRINCE, AND R. A. SPARKS, *J. Appl. Crystallogr.* **16,** 357 (1982).
24. B. RUPP, B. SMITH, AND J. WONG, *J. Appl. Crystallogr.* **24,** 263 (1991).
25. E. KELLER, *J. Appl. Crystallogr.* **22,** 16 (1989).